



# Acoustic detection of the Greenland shark (*Somniosus microcephalus*) using multifrequency split beam echosounder in Svalbard waters

Egil Ona<sup>a</sup>, Julius Nielsen<sup>b,\*</sup>

<sup>a</sup> Institute of Marine Research, P. Box 1870, 5817 Bergen, Norway

<sup>b</sup> Greenland Institute of Natural Resources, P. Box 570, 3900 Nuuk, Greenland

## ARTICLE INFO

### Keywords:

Elasmobranch  
Deep-sea  
Monitoring  
Tracking  
Echogram  
Swimming speed

## ABSTRACT

The conservation status of the long-lived Greenland shark (*Somniosus microcephalus*) is unknown, and methods for non-invasively estimating local or regional abundances are wanted. Using a multifrequency split beam echosounder during long line fishery for Greenland sharks, we demonstrate how individual sharks can be identified and separated with high accuracy from the acoustic backscattering at three frequencies. From a slowly drifting vessel, hooked and free-swimming targets with similar target characteristics were identified on echograms along the bottom and in the water column over a depth of  $\sim 400$  m. A discriminate analysis using target frequency response, target strength and echo pulse stretching was used to identify shark targets from the only possible competitor, with respect to target strength, being large Atlantic cod (*Gadus morhua*). Isolation and tracking of single targets allowed us to calculate the swimming speeds ranging between 0.16 and 0.84  $\text{m s}^{-1}$  (mean  $\pm$  SD,  $0.47 \pm 0.18 \text{ m s}^{-1}$ ) from 15 free-swimming sharks over distances from 11 and 50 m in time periods of 28 to 122 s per track. Our findings demonstrate the first acoustic detection of Greenland sharks, and thus provide a new non-invasive monitoring method applicable in otherwise difficult-to-access arctic and deep-sea waters.

## 1. Introduction

The Greenland shark (*Somniosus microcephalus*) is distributed across the northern North Atlantic Ocean, where it is commonly found throughout the Arctic in deep fjords and offshore waters of the continental shelf and slope (Mecklenburg et al., 2018). With a maximum length of at least 5.5 m (Nielsen, 2018), Greenland sharks are among the largest carnivore sharks in the world and a top predator of Arctic marine food webs, mainly feeding on seals (Pinnipeds) and epibenthic fishes (Leclerc et al., 2012; Nielsen et al., 2019).

In recent years, there has been a growing conservation concern for Greenland sharks (Davis et al., 2013; Kulka et al., 2020) due to the species' age-at-maturity, which for females has been estimated to be  $>100$  years (Nielsen et al., 2016). Official numbers on Greenland shark bycatch levels are believed to be underestimates of the actual bycatch (Davis et al., 2013; Bryk et al., 2018; Edwards et al., 2019; ICES, 2021). The full scale bycatch is likely high in some arctic demersal fisheries exemplified by recently improved logbook reports suggesting a regional Greenland shark bycatch around 2–3% of the targeted biomass for Greenland halibut (*Reinhardtius hippoglossoides*, Greenland Institute of

Natural Resources unpublished data). The only stock assessment conducted for Greenland sharks concluded that the population in the North Atlantic had declined over the past three generations, wherefore the species is listed as 'Vulnerable' on the IUCN Red List of Threatened Species (Kulka et al., 2020).

To conduct a sustainable management of Greenland sharks, it is necessary to know status of the stock. This requires fishery-independent baselines for regional biomass and abundance as well as identification of regions or locations of high density (Davis et al., 2013; Bryk et al., 2018; Devine et al., 2018). Given the scarcity of Greenland sharks caught in scientific demersal trawl surveys (e.g. in Greenland water, see Nielsen et al., 2014), there is a need for novel approaches and techniques to monitor their abundance. Devine et al., (2018) produced the first estimates of local abundance in multiple inshore regions of the Eastern Canadian Arctic, using baited remote underwater video cameras (BRUVs). However, BRUV-based monitoring programs are resource intensive as well as relying on the sharks being attracted to the baited camera. The development of additional observation methods is therefore desirable.

In this study, we present a new technical solution for non-invasively

\* Corresponding author.

E-mail address: [juni@natur.gl](mailto:juni@natur.gl) (J. Nielsen).

<https://doi.org/10.1016/j.pocean.2022.102842>

Received 23 September 2021; Received in revised form 30 May 2022; Accepted 7 June 2022

Available online 15 June 2022

0079-6611/© 2022 The Authors. Published by Elsevier Ltd. This is an open access article under the CC BY license (<http://creativecommons.org/licenses/by/4.0/>).

detecting Greenland sharks using multifrequency split beam echosounders. Based on existing knowledge of acoustic detection of single target backscatter, from fishes without swimbladders (Nakken and Olsen, 1977; Foote, 1980; Korneliussen and Ona, 2002; Simmons and MacLennan, 2005), we investigate the target strength and acoustic characteristics of Greenland sharks on a deep-sea location off Svalbard, Norway. We also evaluated the swimming behavior of otherwise rarely encountered free-swimming Greenland sharks from the acoustic records.

## 2. Materials and methods

### 2.1. Long line deployments

During the SI\_ARCTIC (Strategic Initiative – The Arctic Ocean Ecosystem) 2015 cruise (#2015843, from August 25 to September 9) in the polar basin north of Svalbard, Norway (Ingvaldsen et al., 2016), a demersal long line designed for Greenland sharks, was deployed on a slope over 400–450 m of depth at N 81°02'21''; W17°48'42'' (Fig. 1). The line consisted of 40 stainless steel hooks (Mustad size 4, 5 mm in thickness and 150 mm in height), which were attached to the bottom line with a 70 cm steel chain (chain elements measured 2 mm in thickness and 30 mm in height, Fig. 2). Each hook was baited with either fish or seal blubber and attached to the bottom line, approximately 8 m

apart on the 360 m long line made of nylon rope (8 mm diameter). The bottom line was fixed at each end with 30 kg anchors from which, two headlines to the surface, also were attached. Each headline was 550 m long and made from sinking nylon rope (10 mm diameter). The headlines were attached to 0.4 m<sup>3</sup> buoys at the surface. The effective fishing time of the long line was 12.5 h. The long line operation was conducted under the auspices of the ‘Old & Cold—Greenland shark project’ at the University of Copenhagen, and was carried out in accordance with laws, regulations, and authorization of the Norwegian Fisheries Directorate (No: 14/14305).

### 2.2. Shark handling

Greenland sharks were either measured (total length, TL) in the water from a zodiac (and released with a tag) or brought on deck for more detailed biological sampling to be conducted. On deck, TL was measured more accurately, and body mass recorded using electronic scale. For specimens where TL could not be measured (due to cannibalism from conspecifics), an approximate length ‘~TL’ was calculated according to the formula  $\sim TL = 8.4 \cdot SN + 67.3$  (N = 15, Nielsen unpublished data), where SN is the shortest distance (in centimeter) from the midpoint of the snout to the beginning of the eye.

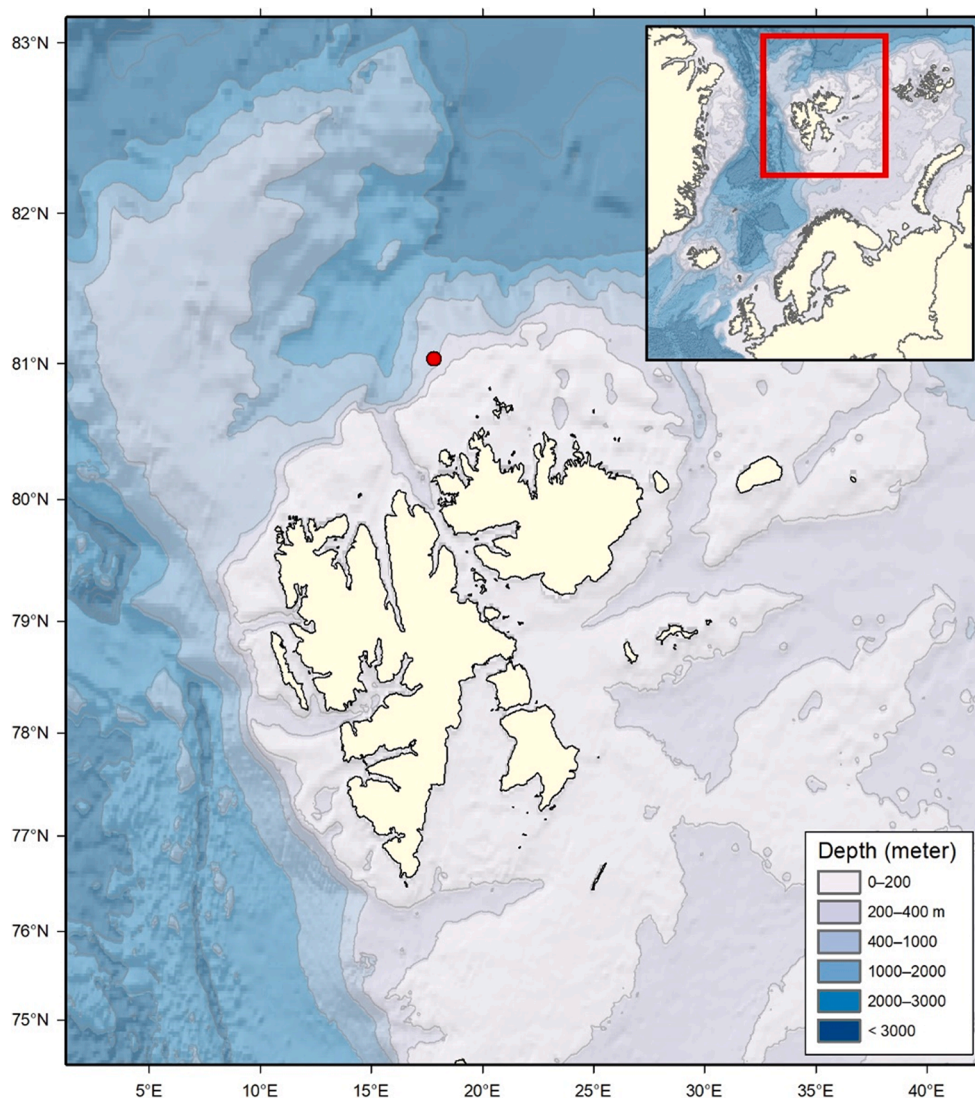


Fig. 1. Location of long line deployment (red dot) north of Svalbard (Norway).

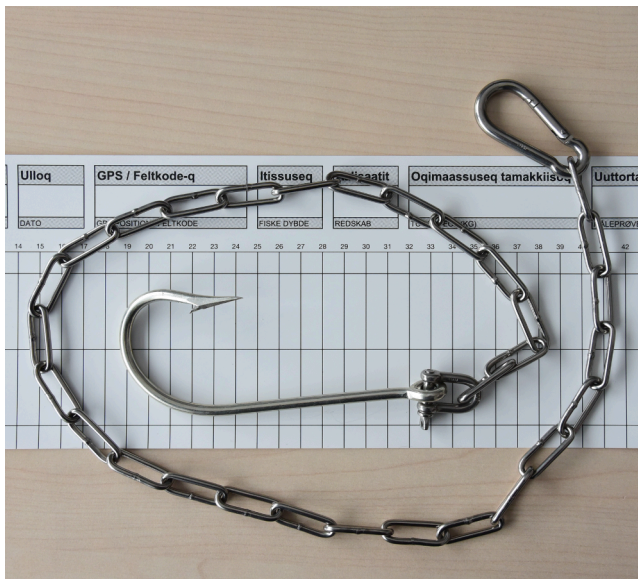


Fig. 2. Stainless steel hook and chain of Mustad size 4, used for catching Greenland sharks on the long line.

### 2.3. Echosounder

Before and during long line retrieval, acoustic measurements were conducted from a nearly stationary vessel (FRV Helmer Hansen, UiT, The Arctic University of Norway) using the vessel's three-frequency Simrad EK60 echosounder (Simrad, 2012) mounted on the drop keel. The echosounder frequencies were 18, 38 and 120 kHz in a split beam configuration with a nominal half power beam width of  $11^\circ$ ,  $7^\circ$  and  $7^\circ$ , respectively. The raw acoustic data was collected to a range of 500 m at a vertical resolution of 0.188 m for all three frequencies. The pulse duration for all frequencies was set at 1.024 ms, and the ping repetition frequency (PRF) was 1.38 Hz, close to the maximum for a 500 m depth. The echosounder calibrations were verified at the start of the survey on 18 August 2015, using a 64 mm tungsten carbide sphere in inshore calm waters (Smeren fjord, Svalbard). Only the split beam performance and on-axis gain,  $G_0$ , was measured, and found to be identical to a larger and more thorough calibration of the vessel transducers at January 2015 (Haugland, 2015).

The echosounder noise level was measured in deep waters at several vessel speeds, as well as with the propeller disconnected, as being used during the stationary measurements. Settings and calibration parameters for each of the echosounders, including the noise level recorded with the sounder in passive mode, is presented in Table 1. Simultaneously, current measurements were made with a RDI 75 kHz Acoustic Doppler Current Profiler (ADCP, <https://www.rdiinstruments.com>), externally triggered by the echosounder. A fixed time delay of about 700 ms was added to the ADCP transmission to prevent acoustic interference on the echosounder data. The resulting PRF on the ADCP was 0.33 Hz, as read from the available ensemble data. Multi-frequency scrutinizing and target strength analysis were conducted using the Large-Scale Survey System (LSSS, version 2.11.0) post processing system (Korneliusen et al., 2006). The results were exported to an external file for further analyses using higher-level programming languages. The ADCP data were read and processed using the RDI software WinADCP.

### 2.4. Data processing

Greenland shark echoes were detected by the echosounders system during long line recovery. The skipper slowly positioned the vessel above the horizontal long lines (marked with two buoys) to enable detection of target signals along the bottom. Several targets were

Table 1

The EK60 echosounder technical specifications and settings employed during the survey.

| EK60 system                                   | 18 kHz  | 38 kHz | 120 kHz  |
|---|---------|--------|----------|
| Transducer Model                              | ES18-11 | ES38B  | ES120-7C |
| Equivalent beam angle $10\log \Psi$ [dB]      | -17.3   | -20.8  | -21      |
| Approximate nearfield range [m]               | 2.4     | 2.8    | 0.9      |
| Calibration Sphere                            | CU-64   | CU-60  | WC38.1   |
| Range to sphere [m]                           | 17      | 17     | 17       |
| Theoretical sphere TS [dB]                    | -34.30  | -33.60 | -39.50   |
| Gain [dB]                                     | 22.33   | 25.53  | 26.69    |
| Sa correction [dB]                            | -0.60   | -0.60  | -0.47    |
| Beam parameters                               |         |        |          |
| Alongship half power opening angle [deg]      | 10.75   | 7.07   | 6.51     |
| Offset Along. Angle [deg]                     | -0.10   | -0.12  | -0.02    |
| Athwartship half power opening angle [deg]    | 10.56   | 7.01   | 6.57     |
| Offset Athwart. Angle [deg]                   | -0.17   | -0.09  | 0.12     |
| Survey settings                               |         |        |          |
| Sound speed [m/s]                             | 1472    | 1472   | 1472     |
| Absorption coefficient [ $\text{dB m}^{-1}$ ] | 0.002   | 0.008  | 0.043    |
| Pulse duration [ms]                           | 1.024   | 1.024  | 1.024    |
| Wavelength [cm]                               | 8.33    | 3.97   | 1.25     |
| Electrical Transmit Power (W)                 | 2000    | 2000   | 250      |
| Transducer positions                          |         |        |          |
| X-alongship location on vessel [m]            | 7.703   | 8.579  | 8.177    |
| Y-athwartship location on vessel [m]          | -0.472  | -0.473 | -0.578   |
| Z-vertical offset [m]                         | 6.19    | 6.169  | 6.176    |
| Vertical Correction [m]                       | -0.15   |        | 0.1      |
| Horizontal Alongship Correction [m]           | -0.87   |        | -0.395   |
| Horizontal Athwartship Correction [m]         |         |        | -0.105   |

detected, which, upon long line retrieval, could be followed towards the surface (Fig. 3). For these targets, the echogram was zoomed in and each single target enclosed in an LSSS "school box". Since the targets were large (TS of  $-15$  to  $-35$  dB re.  $1 \text{ m}^2$ ), the echograms were displayed using an  $S_V$  threshold of  $-70$  dB re.  $1 \text{ m}^2 \text{ m}^{-3}$  and a colour scale limited to  $S_V$  values between  $-50$  and  $-70$  dB re  $1 \text{ m}^2 \text{ m}^{-3}$ . Target strengths were exported from the isolated track, using a minimum TS of  $-35$  dB, and otherwise slightly modified single echo detection filters (SED) for split beam echosounders (Table 2). Other data extracted from the school box was the area scattering coefficient,  $s_A$  ( $\text{m}^2 \text{ nmi}^2$ ), as reported by LSSS inside the "school box" at each of the three frequencies. See examples of LSSS for different targets at the three frequencies in Fig. 4. The thresholded mean volume scattering strength  $S_V$  (dB re  $1 \text{ m}^2 \text{ m}^{-3}$ ) was also recorded, as directly read from the  $S_V$  distribution window. Further, the echo length of the target was first manually read at the  $-20$  dB points relative to the peak, from the LSSS ping plot for the ping with the maximum TS. Later, a more detailed, alternative method was adopted, measuring the effective echo length. Here, the  $S_V$  data of the entire "school box" was stored, and the ping with the maximum TS was identified by its ping number. By summing the linear version of  $S_V$ ,  $sv_i$ , over all samples in the pulse, and dividing by the maximum  $sv$ , the effective echo length was measured by integration:

$$EL_{\text{eff}} = \frac{\sum_i^N sv_i}{sv_{\text{max}}}$$

This procedure was applied for strong targets which presumably encompassed hooked sharks, free-swimming sharks, and free-swimming cod in the same raw data files. The target strength data and split beam positions were used for swimming speed and swimming direction analyses, and the rest of the data for trials on target identification.

The split beam target strength data for an isolated target contains the following parameters: date, time, ship latitude, longitude at each ping, range, beam-corrected target strength, uncorrected target strength, athwartships target angle, and alongship target angle for each detection of the target. Later, data files were manually augmented with vessel roll, pitch, heave, and heading, as exported from the LSSS echogram data viewer. For computing the actual movement of detected free-swimming sharks, the following transformations were made. First the geographical

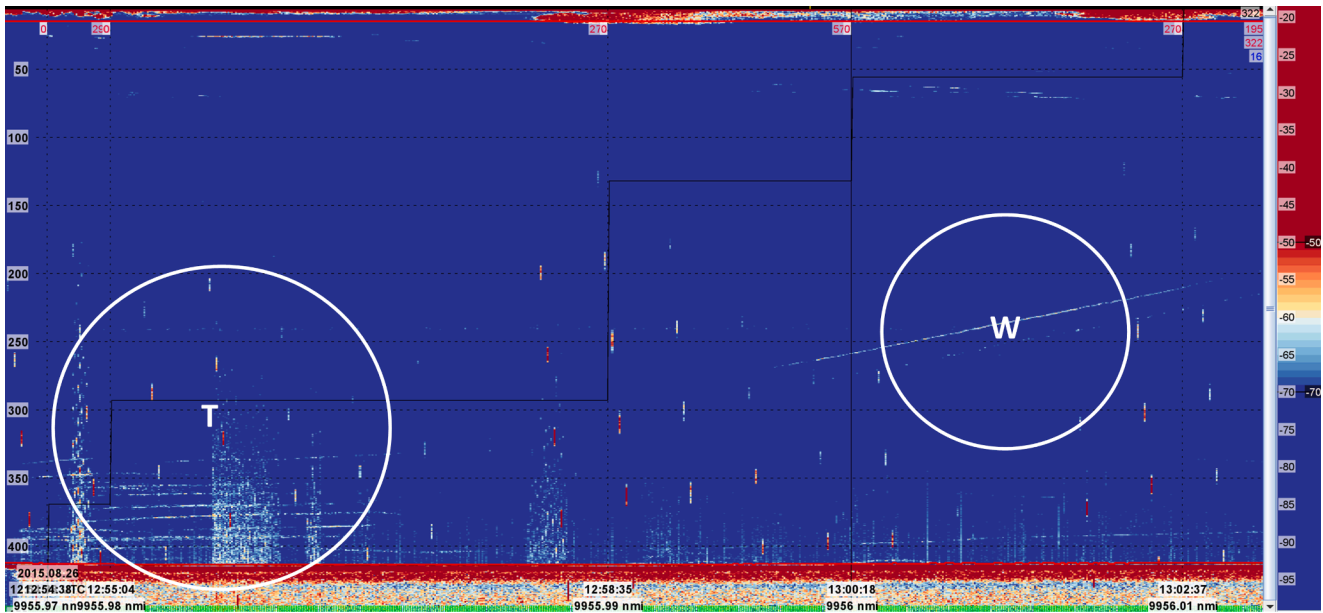


Fig. 3. Screenshot from the LSSS software showing echogram recording on the 120 kHz channel and the first detection of several large targets on the longline (T) and the long line anchor (W) during retrieval, bottom depth 413 m. Some noise from the ADCP transmit pulse and from propeller and machinery is visible.

**Table 2**  
Modified single echo detector settings (nominal value in parenthesis).

| Detector type                            | SED (CW)                   |
|--|----------------------------|
| Minimum TS                               | -35 dB re 1 m <sup>2</sup> |
| Pulse length determination level         | -6.0 dB (-6.0)             |
| Minimum Echo length (rel. 1 ms)          | 0.5 (0.5)                  |
| Maximum Echo length (rel. 1 ms)          | 3.0 (1.8)                  |
| Maximum beam gain compensation (one way) | 6.0 dB (6.0)               |
| Maximum phase deviation                  | 8 steps, (8)               |
| Maximum TS                               | -10 dB re 1 m <sup>2</sup> |

position of the vessel was transformed into the Universal Transverse Mercator (UTM) coordinates to get them into a linear coordinate system. The vessel position is then given as

$$x^v = [x_0^v, \dots, x_i^v, \dots, x_N^v]$$

and

$$y^v = [y_0^v, \dots, y_i^v, \dots, y_N^v],$$

equivalent to the longitude and latitude vessel positions, respectively. Positive y indicates a direction towards north and positive x indicates a direction towards east,  $i$  the  $i^{\text{th}}$  measurement,  $i \in [0, \dots, N]$ , where N is the total number of measurements for each shark. The geographical position of the shark, in the horizontal plane, was expressed by adding the vessel positions  $(x^v, y^v)$  with the positions of the shark relative to the vessel  $(x^{vs}, y^{vs})$ , or more formally,

$$x^s = x^v + x^{vs}$$

and

$$y^s = y^v + y^{vs}$$

Here

$$x^{vs} = [x_0^{vs}, \dots, x_i^{vs}, \dots, x_N^{vs}]$$

and

$$y^{vs} = [y_0^{vs}, \dots, y_i^{vs}, \dots, y_N^{vs}]$$

The shark positions relative to the vessel  $(x^{vs}, y^{vs})$  are not given directly through the data and were computed using the transducer split beam position compensated by the vessel's heading, pitch and roll as shown in the following section.

The split beam system could detect the direction of single targets within a conical observation volume of 10° opening angle beneath the vessel. The target direction is given by the athwartships angle ( $\alpha$ ), positive to starboard, and the alongship angle ( $\beta$ ). See Ona (1999) for more details. The target's  $i^{\text{th}}$  position, on a horizontal plane relative to the vessel, is

$$x'_i = r_i \tan(\alpha_i - \theta_i)$$

and

$$y'_i = r_i \tan(\beta_i - \phi_i)$$

Here  $r_i$  is the range to the target,  $\theta_i$  and  $\phi_i$  the vessel's roll and pitch angle, respectively, at the same time as the  $i^{\text{th}}$  detection.  $\phi = 0$  when the vessel is horizontally aligned with the sea surface in the athwart ship direction, with positive angles when the bow is moving upwards. Similar with  $\theta$ , where positive angles are towards port side of the vessel. If the vessel's Motion Reference Unit (MRU) is mounted close to the transducer, these angles may be summed directly to the split beam directions for simplicity. However, if the MRU is not located close to the transducer, the pitch and roll angles, including vessel heave, need to be corrected, as it is done in advanced multibeam bottom mapping systems (Lekkerker and Theijs, 2011). The ' in  $x'_i$  and  $y'_i$  indicate that the position is relative to a coordinate system, where positive  $y'_i$  indicates a direction along the vessel, and  $x'_i$  indicates direction towards starboard side. These coordinates may be transformed to the UTM coordinate system using

$$x_i^{vs} = x'_i \cos(-\psi_i) - y'_i \sin(-\psi_i)$$

and

$$y_i^{vs} = x'_i \sin(-\psi_i) + y'_i \cos(-\psi_i)$$

Here  $\psi_i$  is the vessel's heading at the  $i^{\text{th}}$  measurement. The track of each shark in absolute coordinates was used to plot its movement and to calculate the mean swimming speed. Rather than computing this from

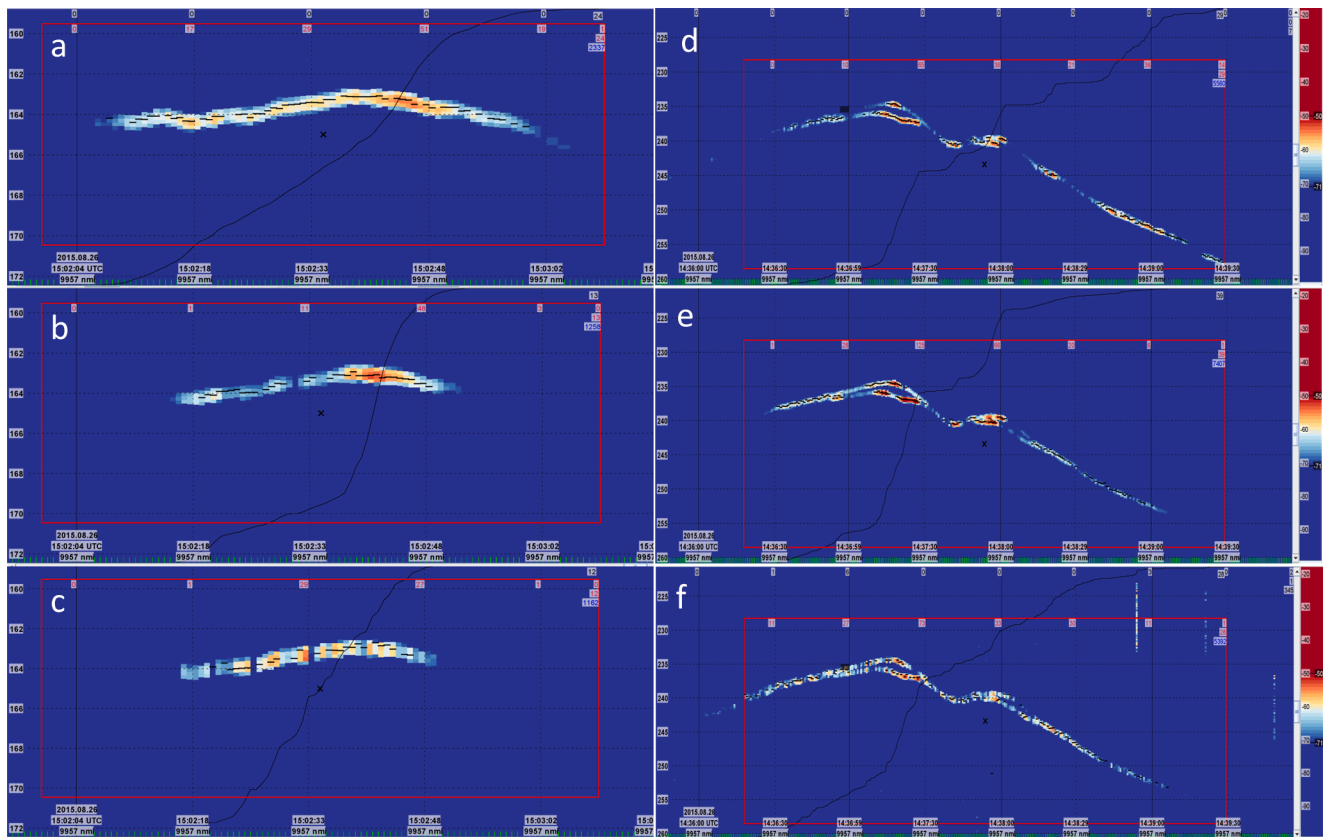


**Fig. 4.** Track of Atlantic cod (a, b and c) at 165 m and of two free-swimming sharks (d, e and f) at 240 m depth. The frequencies are 18 kHz (a, d), 38 kHz (b, e) and 120 kHz (c, f) thresholded at  $S_v = -70$  dB. Time along the X-axis and distance between pings as green markers. Black marks inside track indicate valid TS detections during the track. Mean area scattering coefficient,  $s_A$  in red numbers in right corner of the red school box.

individual detections, the distance moved from first to last detection, was used to estimate the swimming speed. The swimming direction was calculated in a similar way (i.e., the direction from the first to last detection). The current speed and direction of the surrounding water mass was obtained from the ADCP data as an average over 1-minute period in a 20-meter-wide layer at the same depth as the shark.

To ensure that the free-swimming targets were from Greenland sharks, the maximum track target strength, the relative frequency response of the track at 18, 38, and 120 kHz, and echo length were extracted for each target in the strongest part of the echo track at 38 kHz. Two frequency response values were tried. First, the frequency response, as defined by Korneliusson and Ona (2002),

$$r(f) = \frac{sv_f}{sv_{38}},$$

was used, as directly read from the LSSS frequency response window. An alternative version of the frequency response (Johnsen et al., 2009) was also tried since the first version was limited when only three frequencies were used, when normalized to the backscattering at 38 kHz. The alternative one was.

$$ro(f) = \frac{s_A(f)}{\sum_3 s_A(f)},$$

which measures the relative contribution from one frequency compared to the sum. When using three frequencies  $ro(f) = 0.33$  indicates a flat frequency response. The summed area scattering coefficient was used to scale the mean backscattered strength.

The data from hooked and free-swimming sharks were further compared with several echoes from the only targets of comparable target strength in the survey area being large specimens of Atlantic cod.

Echoes from cod are expected to have a different frequency response due to their gas-filled swimbladder being the dominant sound reflector. For Greenland sharks, the main reflector is expectedly their large liver and surrounding large body (Foote, 1980). The echoes from Greenland shark were tried separated from Atlantic cod echoes using a simple discriminant analysis (Systat Inc, 1992) for three target categories: 1) free-swimming sharks, 2) free-swimming cod, or 3) Greenland sharks hooked on the long line.

To calculate swimming speed of free-swimming Greenland sharks the movements of the vessel (roll, pitch, and heave) have been subtracted from the apparent movement of the fish, as determined from the split beam phase angles to the target in each ping. The drifting of the vessel was further subtracted from the GPS position of the vessel in each ping. Since the track data was geo-referenced, the remaining movement is the swimming speed of the fish, independent of ocean current speed. The calm weather resulted in very little vessel movement which added only a slight jitter to the movement data and consequently, compensation for vessel heave, pitch, and roll had little effect on the main tracking results (Table 3).

**Table 3**  
Typical vessel movement during 100 ping track no. 1417.

| Parameter      | Mean value | Standard deviation |
|----------------|------------|--------------------|
| Heading (Deg.) | 315        | 2.54               |
| Heave (m)      | 0.0        | 0.052              |
| Pitch (Deg.)   | 2.89       | 0.201              |
| Roll (Deg.)    | -1.24      | 0.139              |

### 3. Results

Twenty Greenland sharks were caught on the long line measuring between 2.7 and 3.6 m TL with a body mass from 154 to 356 kg (Table 4). Sex and liver weight were also recorded when possible. Fourteen sharks had distinct bitemarks with a characteristic cutting edge evidencing that these were made by conspecifics (Fig. 5). Due to missing body parts and intestines, body mass, liver weight and TL could occasionally not be measured. Therefore not all sharks on the line were suitable for acoustic measuring.

From interpretation of the echo recordings made during long line retrieval, the anchors on the long line rig were detected and registered together with a series of well-defined targets hooked on the long line (Fig. 3). The distance between several of these targets was about 8 m, matching the hook distance on the long line. The targets remained visible while the long line was retrieved towards the surface (Fig. 6a) and had a target strength of  $-30$  dB re  $1 \text{ m}^2$  or stronger at 38 kHz. Such a strong reflection is expected from very large fish without a swimbladder (such as a Greenland shark) at or close to broadside aspect. The physical height of the target also appears to stretch the backscattered echo (Ona and Mitson, 1996) due to the substantial height or diameter of the body. Having identified several individual targets on the long line during retrieval, further inspection of the water column for similar strong targets, revealed several tracks of free-swimming sharks. These were both close to the bottom, and in the pelagic region, 10–170 m above the bottom (Fig. 6b-d). Magnifying the recordings and refining the target detection algorithm, allowed for the detection of well-defined single target traces with target strength values, that were expected for shark targets, but naturally varying with target orientation. A total of 15 free-swimming sharks were visually spotted on the echograms at depths between 157 m and 382 m (mean  $\pm$  SD,  $304 \pm 57$  m) in the surrounding one nautical mile on each side of the retrieval point. Numerous smaller targets, swimbladdered fish, with target strengths from  $-45$  to  $-35$  dB re  $1 \text{ m}^2$ , were also observed, but omitted from this analysis. The Greenland shark maximum target strength at 38 kHz was between  $-16$  and  $-26$  dB re  $1 \text{ m}^2$ , with a mean track TS of  $-28.1$  dB re  $1 \text{ m}^2$ . The standard deviation inside each track was about 3.5 dB using a hard minimum TS threshold ( $-35$  dB) in the single target echo detector (Table 2). The frequency response of the observed targets (measuring the animal echo reflection properties in the frequency domain, Fig. 7a) and the general appearance of the echo traces, were more similar to echoes of large targets without a swimbladder than for fish with a gas-filled swimbladder (Ona, 1990). The response indicates, that the

**Table 4**

Information on body metrics and sex for all sharks caught on the long line. For individuals where total length could not be measured,  $\sim$ TL was estimated.

| No | ID    | TL (m)     | Sex | Body mass (kg) | Liver weight (kg) |
|----|-------|------------|-----|----------------|-------------------|
| 1  | GS189 | $\sim$ 3.5 | ?   | –              | –                 |
| 2  | GS190 | $\sim$ 3.4 | ?   | –              | –                 |
| 3  | GS191 | 3.40       | M   | –              | –                 |
| 4  | GS192 | $\sim$ 3.1 | ?   | –              | –                 |
| 5  | GS193 | $\sim$ 3.1 | ?   | –              | –                 |
| 6  | GS194 | 3.47       | M   | –              | 65.1              |
| 7  | GS195 | 2.77       | F   | 154            | 13.5              |
| 8  | GS196 | 3.12       | F   | 230            | 22.7              |
| 9  | GS197 | 3.08       | M   | 290            | 36.0              |
| 10 | GS198 | 3.06       | F   | 220            | 22.6              |
| 11 | GS199 | 3.22       | F   | 273            | 31.0              |
| 12 | GS200 | 3.48       | F   | 356            | 46.9              |
| 13 | GS201 | 2.90       | M   | –              | –                 |
| 14 | GS202 | 3.60       | F   | –              | –                 |
| 15 | GS203 | 3.20       | M   | –              | –                 |
| 16 | GS204 | 3.00       | M   | –              | –                 |
| 17 | GS205 | 2.97       | M   | –              | –                 |
| 18 | GS206 | 2.94       | F   | –              | –                 |
| 19 | GS207 | 2.77       | M   | –              | –                 |
| 20 | GS208 | 2.70       | M   | –              | –                 |

hooked targets have a larger difference and variability at three frequencies, than what is observed between free-swimming sharks and cod. The reason for this is not obvious, but the response at 120 kHz may be more affected by the unwanted echo-contribution from the steel chains and hooks on the longline, than the echoes at the lower frequencies. It is also observed that echoes from the empty hooks and chains are best observed between the individual shark targets on the long line at the 120 kHz system. The expected frequency response curve for single targets of cod (Pedersen & Korneliussen 2009), using 5 frequencies in the Lofoten grounds, is straighter and steeper, being stronger at 18 kHz, and weaker at 120 kHz than for the few cod targets observed here. Additional parameters, like targets strength and echo length must therefore be used when trying to discriminate between the categories as shown in Fig. 7. The discriminant analysis, indicated that hooked sharks, are readily separated from free-swimming sharks and cod. Discrimination between free-swimming sharks and cod is less accurate (Fig. 7b, Table 6).

At three occasions, free-swimming sharks were composed by two targets showing a synchronous swimming pattern with respect to direction, swimming speed and depth change. For these observations, target strengths were similar indicating similar-sized sharks. The distance between them (undulating between 1 m and 4 m), suggested that they were swimming pairwise (Fig. 6c and d). Detailed, manual separation of the two tracks can be done from the split beam data on the parts of the track, to study the two trajectories in 3D in the periods of separation. For example, for the sharks in Fig. 6c, the maximum separation in the horizontal dimension is  $0.7^\circ$ , corresponding to 2.8 m at 230 m depth, occurring when the maximum vertical distance between the two was 1.9 m. Since their undulating, paired swimming lasts over 160 s inside the acoustic beams, the mean swimming speeds were identical, and the sharks were indeed swimming pairwise. Using split beam target tracking algorithms, the swimming speed of free-swimming Greenland sharks was estimated to be from  $0.16$  to  $0.84 \text{ m s}^{-1}$  (mean  $\pm$  SD,  $0.47 \pm 0.18 \text{ m s}^{-1}$ ) measured over distances of 11 m to 50 m during time periods of 28 to 122 s per track (Table 5). The average swimming direction of these sharks was  $91.5 \pm 112^\circ$  and the current direction and speed was  $192 \pm 10^\circ$  and  $0.175 \pm 0.025 \text{ m/s}$ , respectively.

### 4. Discussion

During one long line set intended for Greenland sharks, the acoustic records from a multifrequency split beam echosounder were scrutinized, to evaluate if detection of sharks was possible. As the line had caught 20 sharks, the catch was suitable for the purpose although several sharks where partly eaten by conspecifics.

The first detections of sharks on the longline was more difficult to analyze than subsequently detecting free-swimming sharks. This because, despite the hooked sharks on the long line were clear and strong targets, the steel hooks and chains are good acoustic reflectors. This can disturb the target strength algorithm, as well as the echo amplitude at the different frequencies. A preliminary analysis of echo levels between the large approaching free-swimming sharks and the hooked sharks indicated, that hook and chain had a target strength level of about  $-45$  dB re  $1 \text{ m}^2$  at 38 kHz, and that they are more directive at the higher frequency, 120 kHz. The strong targets of hooked sharks were thus 10 to 20 dB's stronger than the chain echoes, and were not expected to be severely affected. However, the frequency response of free-swimming sharks are considered to be more accurate than those hooked on the line. In addition, the hooked targets on the long line, were on occasion only part of a shark, as predation from conspecifics was observed. If any of these were detected and analyzed as whole fish, the real target strength may be underestimated, and the frequency response misleading. It was expected that the frequency response would differ more between free-swimming sharks and cod than what was actually observed – both having nearly the same shape, with a drop towards higher frequencies. Compared to the expected frequency response for



Fig. 5. Greenland shark from a long line with a distinct circular bite wound from a conspecific.

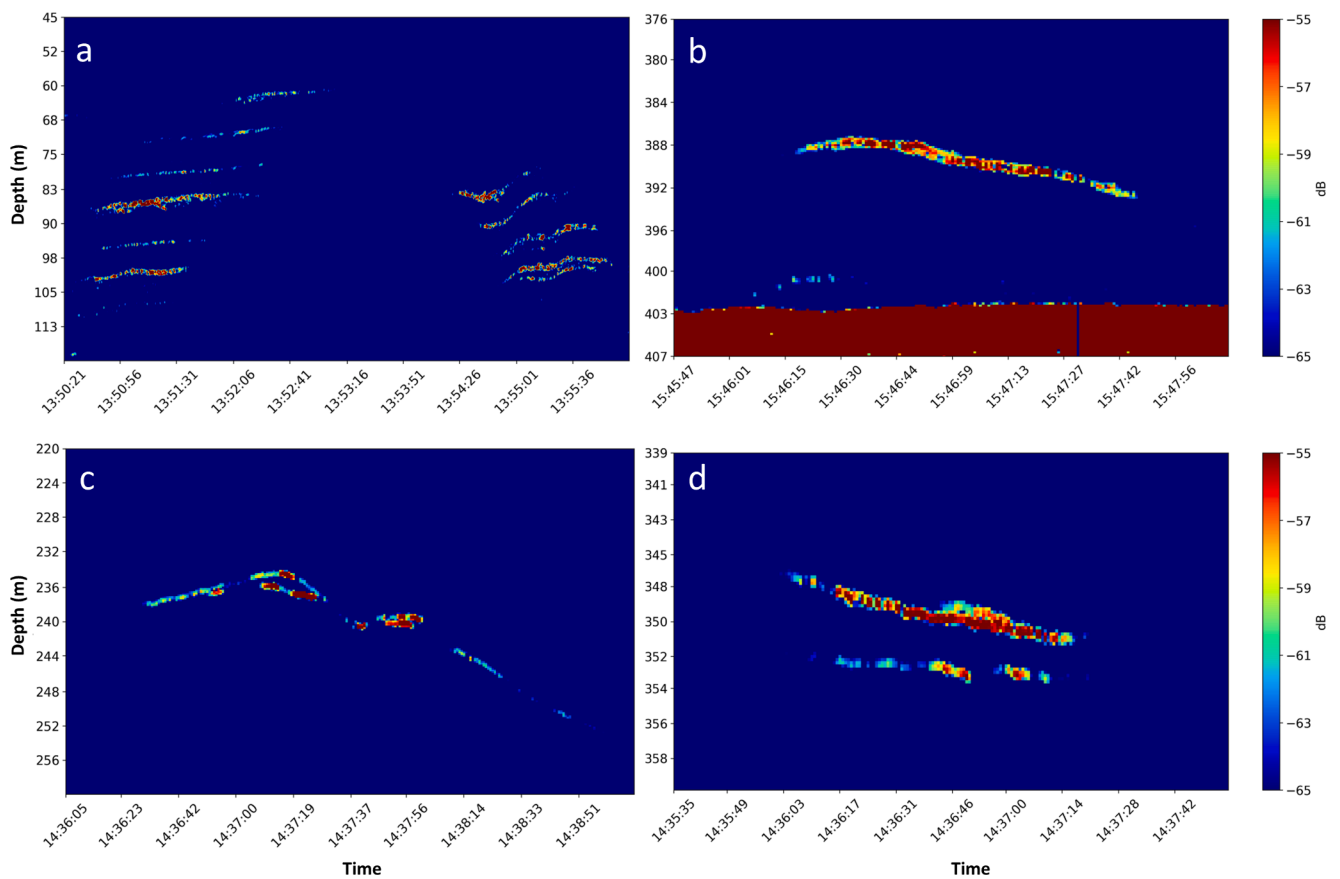


Fig. 6. **a:** Echogram at 120 kHz of several targets in the water column presumably hooked on a long line during retrieval. The targets had similar distance to each other matching the hook distance of ~ 8 m. **b-d:** Echograms at 38 kHz showing single and pairwise free-swimming targets in the water column near the long line. Pairwise targets exhibited 0 to 5 m distance between each other.

cod (as reported in Pedersen and Korneliussen (2009)) and our own experience from the Lofoten spawning ground surveys in northern Norway), the curves obtained in this study, were too flat to resemble that of cod. However, with only visual inspection of the raw echograms and no supporting catch information, there is a chance that a small Greenland shark could be misinterpreted as a cod. Nevertheless, we are convinced, that the bulk of the Greenland shark tracks are correctly interpreted. We also know from earlier use of discriminant analysis, that bringing only one “enemy” into the wrong dataset, may easily destroy the overall statistics when dataset is small, as it the case in this study.

The echo length of the target measured at -20 dB level relative to the peak was used in the discriminant analysis, rather than the effective echo length. This because it was more different especially between free-swimming sharks and cod ( $P < 0.001$ , KW two sample test), while barely significantly different between hooked and free-swimming sharks ( $P = 0.05$ ). This probably means that the pulse stretching is caused by the muscle tissue of the shark target, rather than by the main reflection, which is assumed to be the liver in this rather complex target.

From the findings presented here, it is demonstrated that acoustic detection of Greenland shark using multifrequency split beam

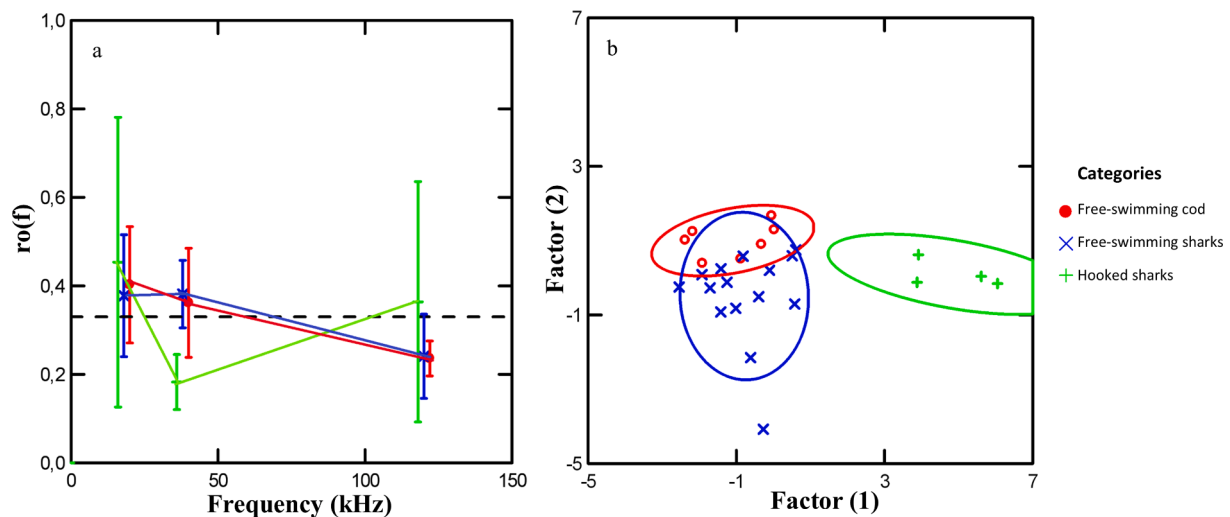


Fig. 7. a: Frequency response,  $ro(f)$  for free-swimming cod (red), free-swimming sharks (blue) and hooked sharks (green). A flat response (same echo energy) for the three frequencies is indicated by the 0.33 level. b: Canonical scores plot from the discriminant analysis with the same three categories.

Table 5  
Overall track data of 15 free-swimming Greenland sharks between 13:00 to 16:00 on 26.08.2015.

| Track # | Speed ( $ms^{-1}$ ) | Distance (m) | Detections (n) | Direction (Deg.) | Range (m) | $TS_{max}$ (dB re $1 m^2$ ) | $\langle TS \rangle$ (dB re $1 m^2$ ) | $TS_{SD}$ (dB) | Track ID    |
|---------|---------------------|--------------|----------------|------------------|-----------|-----------------------------|---------------------------------------|----------------|-------------|
| 1       | 0.58                | 50           | 88             | 334              | 342       | -16.8                       | -23.1                                 | 3.6            | 1436upper   |
| 2       | 0.61                | 48           | 78             | 303              | 346       | -21.4                       | -28.5                                 | 3.7            | 1436lower   |
| 3       | 0.16                | 11           | 66             | 18               | 228       | -24.0                       | -32.9                                 | 3.8            | 1437left    |
| 4       | 0.54                | 22           | 42             | 78               | 233       | -22.5                       | -32.0                                 | 2.5            | 1437upper   |
| 5       | 0.52                | 44           | 42             | 43               | 332       | -19.0                       | -25.0                                 | 3.8            | 1457        |
| 6       | 0.24                | 18           | 75             | 270              | 312       | -24.5                       | -28.2                                 | 2.9            | 1427        |
| 7       | 0.41                | 30           | 72             | 30               | 317       | -22.9                       | -27.8                                 | 2.8            | 1616        |
| 8       | 0.27                | 16           | 59             | 16               | 294       | -22.2                       | -28.2                                 | 4.5            | 1546        |
| 9       | 0.61                | 47           | 78             | 47               | 382       | -18.8                       | -22.5                                 | 2.5            | 1546deep    |
| 10      | 0.84                | 24           | 28             | 23               | 157       | -26.6                       | -32.7                                 | 5.2            | 1515shallow |
| 11      | 0.66                | 18           | 28             | 18               | 333       | -22.9                       | -27.8                                 | 3.8            | 1303deep    |
| 12      | 0.40                | 49           | 122            | 95               | 317       | -24.3                       | -28.7                                 | 3.5            | 1407left    |
| 13      | 0.30                | 22           | 73             | 23               | 320       | -22.0                       | -26.4                                 | 2.3            | 1407right   |
| 14      | 0.43                | 30           | 71             | 30               | 328       | -24.9                       | -28.7                                 | 3.5            | 1417left    |
| 15      | 0.51                | 50           | 98             | 45               | 327       | -23.6                       | -29.3                                 | 4.4            | 1417Right   |

Table 6  
Classification Matrix from simple SYSTAT Discriminant analysis, Categories used: ‘Shark, free-swimming’; ‘Shark, hooked’ and ‘Cod, free-swimming’.

|                      | Shark, free-swimming | Shark, hooked | Cod, free-swimming | % CORRECT |
|----------------------|----------------------|---------------|--------------------|-----------|
| Shark, free-swimming | 10                   | 0             | 5                  | 67        |
| Cod, free-swimming   | 0                    | 0             | 7                  | 100       |
| Shark, hooked        | 0                    | 4             | 0                  | 100       |
| TOTAL                | 10                   | 4             | 12                 | 81        |

echosounders is possible. At a minimum, the method can detect Greenland sharks of around 2 m in length (or larger) at depths down to at least 400 m. Although Greenland sharks have been reported at depths of 2.9 km (Porteiro et al., 2017), tagging studies have shown a preferred swimming depth of 200–400 m in some high-arctic regions (Fisk et al., 2012; Campana et al., 2015). Therefore, we suggest that Greenland sharks can be detected in acoustic surveys of commercial pelagic species such as capelin (*Mallotus villosus*), mackerel (*Scomber scombrus*), herring (*Clupea harengus*) and blue whiting (*Micromesistius poutassou*), which are conducted in inshore and offshore Arctic shelf waters. Ideally, by developing proper identification algorithms on single track data at several frequencies, assisted by the use of artificial intelligence (AI)

(Brautaset et al., 2020), the acoustic method can be used to estimate the abundance of Greenland sharks with a minimum of additional effort. Furthermore, the development and use of broad band split beam echosounder systems (Andersen et al., 2013; Lavery et al., 2017; Simrad, 2012) may facilitate more accurate target identification through spectral analysis of the echo and the increased range resolution compared to the narrowband echosounder system used in this study. In particular, the echo pulse stretching part of the analysis would be simpler and more accurate (Kubilius et al., 2020) and may be feasible for size estimation of well-tracked sharks. Regardless of methodological improvements, this acoustic method has the potential in the future, to identify regions of high Greenland shark concentration. In combination with data obtained from other methods such as BRUVs, acoustics could be a useful tool for developing regional baseline levels of abundance, which are pivotal to evaluate the regional impact of fisheries on Greenland sharks in the Arctic.

The findings of this study also provide information on the biology and swimming behavior of Greenland sharks. First, the presence of multiple free-swimming sharks in the vicinity of the long line combined with multiple hooked sharks having lethal injuries caused by conspecifics (Fig. 5), demonstrates the opportunistic feeding behavior of Greenland sharks. It must be noted that, although cannibalism among Greenland sharks caught on stationary fishing gear is commonly observed (MacNeil et al., 2012, J. Nielsen pers obs.), such feeding



behavior is not of dietary importance for the Greenland shark (see prey items in Yano et al., 2007, McMeans et al., 2010, Leclerc et al., 2012, and Nielsen et al., 2019). The detection of free-swimming sharks up to 170 m above the bottom is strong evidence of a pelagic swimming behaviour, which also has been described in previous tagging studies (Skomal and Benz, 2004; Campana et al., 2015). However, as these observations were made during and after retrieval of the long line, we cannot rule out that the sharks were attracted upwards from the bottom to the water column and hence their pelagic presence there were not natural. A pelagic swimming behaviour do however coincides with the morphological structure of the Greenland shark olfactory organ, which resembles that of benthopelagic sharks (Ferrando et al., 2016). That being said, the most dominant fish prey items for Greenland sharks do not include pelagic fishes but rather demersal and epibenthic species, which supports that active hunting for fish mostly occurs along the ocean floor (Leclerc et al., 2012; Nielsen et al., 2019). Seals however, are also important prey and suspected to be hunted while resting in the water (Leclerc et al., 2012). From the acoustic recordings, it was also shown that the swimming direction of free-swimming sharks was mostly against the current and towards the long line. It is likely that the sharks were attracted by the scent from the baited long line, include live and dead sharks. Swimming speeds of these sharks ranged between 0.16 m s<sup>-1</sup> to 0.84 m s<sup>-1</sup>, which are in consistency with swimming speeds of 0.1 m s<sup>-1</sup> to 1.4 m s<sup>-1</sup> visually estimated by scuba divers of undisturbed Greenland sharks (N = 10, Harvey-Clark et al., 2005). It also coincides with estimates obtained from Greenland sharks tagged with accelerometers (N = 6, mean = 0.37 m s<sup>-1</sup>, max = 0.74 m s<sup>-1</sup>, Watanabe et al., 2012). On several occasions, the acoustic tracks revealed Greenland sharks in pairwise swimming. For example, two tracked sharks had the same swimming speed and direction and were no more than 2.8 m from each other (Fig. 6c) Pairwise swimming has also been observed a single time by scuba divers (Harvey-Clark et al., 2005). Interestingly, from 25 years of bottom trawl survey, approximately one third of all Greenland sharks (N<sub>total</sub> = 123) have been caught in groups of two or more (range 2–6 sharks per haul, GINR unpublished data). Given these observations, pairwise (or group) swimming may be more common for Greenland sharks than currently described in the literature – a behavior which could increase their directive sensitivity for smell detection (Nosal et al., 2016) and thus be advantageous, for example, when searching for food.

The findings presented here provide a novel tool for non-invasive detection of Greenland sharks in the upper 400 m of the water column. They provide insights into the biology of Greenland sharks and support existing estimates of swimming speed, opportunistic feeding behavior, and suggest that pelagic swimming behavior is common. The pelagic behavior highlights the potential relevance of using acoustic monitoring systems for detecting regions of high abundance of Greenland sharks.

#### CRediT authorship contribution statement

**Egil Ona:** Conceptualization, Data curation, Formal analysis, Funding acquisition, Investigation, Methodology, Project administration, Resources, Software, Supervision, Validation, Visualization, Writing – original draft. **Julius Nielsen:** Conceptualization, Data curation, Project administration, Supervision, Visualization, Writing – original draft.

#### Declaration of Competing Interest

The authors declare that they have no known competing financial interests or personal relationships that could have appeared to influence the work reported in this paper.

#### Acknowledgements

The authors are grateful to the crew and captain of FRV Helmer Hansen, The Arctic project (under which the data were collected), IMR

for support, and Dr. Guosong Zhang (IMR) for helping with the figures. The study received financial support from the Research Council of Norway through the project “Strategic Initiative –the Arctic Ocean Ecosystem” – (SI\_ARCTIC, RCN 228896), and the Center for Research-based Innovation in Marine Acoustic Abundance Estimation and Backscatter Classification (CRIMAC) (Project No. 309512) (www.crimac.no). The study was also supported by ‘Old & Cold—Greenland shark project’ at the University of Copenhagen (<http://bioold.science.ku.dk/jfsteffensen/OldAnd-Cold/>) and by the TUNU-Programme at UiT The Arctic University of Norway. We thank two reviewers and Dr. Gavin Macaulay for their valuable comments and suggestions which improved the quality of the paper.

#### References

- Andersen, L.N., Ona, E., Macaulay, G., 2013. Measuring fish and zooplankton with a broadband split beam echosounder. In 2013 MTS/IEEE OCEANS - Bergen, pp. 1–4.
- Brautaset, O., Waldeland, A.U., Johnsen, E., Malde, K., Eikvil, L., Salberg, A.B., Handegard, N.O., 2020. Acoustic classification in multifrequency echosounder data using deep convolutional neural networks. *ICES J. Mar. Sci.* 77, 1391–1400.
- Bryk, J.L., Hedges, K.J., Treble, M.A., 2018. Summary of Greenland Shark (*Somniosus microcephalus*) catch in Greenland Halibut (*Reinhardtius hippoglossoides*) fisheries and scientific surveys conducted in NAFO Subarea 0. NAFO SCR Doc. 18/041. Serial No. N6831. 1–20 pp.
- Campana, S.E., Fisk, A.T., Klimley, A.P., 2015. Movements of Arctic and northwest Atlantic Greenland sharks (*Somniosus microcephalus*) monitored with archival satellite pop-up tags suggest long-range migrations. *Deep-Sea Research Part II* 115, 109–115.
- Davis, B., VanderZwaag, D.L., Cosandey-Godin, A., Hussey, N.E., Kessel, S.T., Worm, B., 2013. The conservation of the Greenland Shark (*Somniosus microcephalus*): setting scientific, law, and policy coordinates for avoiding a species at risk. *J. Int. Wildlife Law & Policy* 16, 300–330.
- Devine, B.M., Wheeland, L.J., Fisher, J.A.D., 2018. First estimates of Greenland shark (*Somniosus microcephalus*) local abundances in Arctic waters. *Sci. Rep.* 8 (1) <https://doi.org/10.1038/s41598-017-19115-x>.
- Edwards, J.E., Hiltz, E., Broell, F., Bushnell, P.G., Campana, S.E., Christiansen, J.S., Devine, B.M., et al., 2019. Advancing research for the management of long-lived species: a case study on the Greenland shark. *Front. Mar. Sci.* 6.
- Ferrando, S., Gallus, L., Ghigliotti, L., Vacchi, M., Nielsen, J., Christiansen, J.S., Pisano, E., 2016. Gross morphology and histology of the olfactory organ of the Greenland shark *Somniosus microcephalus*. *Polar Biol.* 39, 1399–1409.
- Fisk, A.T., Lydersen, C., Kovacs, K.M., 2012. Archival pop-off tag tracking of Greenland sharks *Somniosus microcephalus* in the high Arctic waters of Svalbard, Norway. *Marine Ecology Progress Series* 468, 255–265.
- Foote, K.G., 1980. Importance of the swimbladder in acoustic scattering by fish: A comparison of gadoid and mackerel target strengths. *J. Acoustical Soc. Am.* 67.
- Harvey-Clark, C.J., Gallant, J.J., Batt, J.H., 2005. Vision and its relationship to novel behaviour in St. Lawrence River Greenland Sharks, *Somniosus microcephalus*. *Canadian Field-Naturalist* 119, 355–358.
- Haugland, T., 2015. Instrument report RV Helmer Hansen. Cruise no: 2015841, January 20 - February 16, 2015. (In Norwegian). Extracted from; raw survey data depository at the Norwegian Marine Data Center, NMD, (\ces\cruise\_data\2015\S2015841\_PHELMERHANSEN 1173). Bergen, Norway.
- ICES, 2021. Working Group on Elasmobranch Fishes (WGEF). 789 pp. [http://www.ices.dk/sites/pub/Publication Reports/Expert Group Report/Fisheries Resources Steering Group/2020/WGEF/01 WGEF Report 2020.pdf](http://www.ices.dk/sites/pub/Publication%20Reports/Expert%20Group%20Report/Fisheries%20Resources%20Steering%20Group/2020/WGEF/01%20WGEF%20Report%202020.pdf).
- Ingvaldsen, R.B., Bucklin, A., Chierici, M., Gjøsæter, H., Haug, T., Hosa, A., Jørgensen, L. L., et al., 2016. Cruise report SI\_ARCTIC/Arctic Ecosystem survey R/V Helmer Hansen, 17 August-7 September 2015. 45 pp.
- Johnsen, E., Pedersen, R., Ona, E., 2009. Size-dependent frequency response of sandeel schools. *ICES J. Mar. Sci.* 66, 1100–1105.
- Korneliussen, R.J., Ona, E., 2002. An operational system for processing and visualizing multi-frequency acoustic data. *ICES J. Mar. Sci.* 59, 293–313.
- Korneliussen, R.J., Ona, E., Eliassen, I.K., Heggelund, Y., Patel, R., Godø, O.R., Giertsen, C., et al., 2006. The Large Scale Survey System - LSSS. Proceedings of the 29th Scandinavian Symposium on Physical Acoustics, 29: 6.
- Kubilius, R., Macaulay, G.J., Ona, E., 2020. Remote sizing of fish-like targets using broadband acoustics. *Fish. Res.* 228, 105568.
- Kulka, D.W., Cotton, C.F., Andersen, B., Derrick, D., Herman, K., Dulvy, N.K., 2020. *Somniosus microcephalus*. The IUCN Red List of Threatened Species 2020, e.T60213A1.
- Lavery, A.C., Bassett, C., Lawson, G.L., Jeck, M., 2017. Exploiting signal processing approaches for broadband echosounders. *ICES J. Mar. Sci.* 74, 2262–2275.
- Leclerc, L.M.E., Lydersen, C., Haug, T., Bachmann, L., Fisk, A.T., Kovacs, K.M., 2012. A missing piece in the Arctic food web puzzle? Stomach contents of Greenland sharks sampled in Svalbard, Norway. *Polar Biol.* 35, 1197–1208.
- Lekkerker, H.J., Theijs, M.J., 2011. Handbook of offshore surveying. Skilltrade, Voorschoten.
- MacNeil, M.A., McMeans, B.C., Hussey, N.E., Vecsei, P., Svavarsson, J., Kovacs, K.M., Lydersen, C., et al., 2012. Biology of the Greenland shark *Somniosus microcephalus*. *J. Fish Biol.* 80, 991–1018.

- McMeans, B.C., Svavarsson, J., Dennard, S., Fisk, A.T., 2010. Diet and resource use among Greenland sharks (*Somniosus microcephalus*) and teleosts sampled in Icelandic waters, using  $\delta^{13}\text{C}$ ,  $\delta^{15}\text{N}$ , and mercury. *Can. J. Fish. Aquat. Sci.* 67, 1428–1438.
- Mecklenburg, C.W., Lynghammar, A., Johannesen, E., Byrkjedal, I., Christiansen, J.S., Karamushko, O.V., Mecklenburg, T.A., et al., 2018. Marine fishes of the Arctic region. *Akureyri*. 731, pp.
- Nakken, O., Olsen, K., 1977. Target-strength measurements of fish. *Rapports et Procès-Verbaux des Reunions du Conseil International pour l'Exploration de la Mer* 170, 52–69.
- Nielsen, J., Hedeholm, R.B., Simon, M., Steffensen, J.F., 2014. Distribution and feeding ecology of the Greenland shark (*Somniosus microcephalus*) in Greenland waters. *Polar Biol.* 37, 37–46.
- Nielsen, J., Hedeholm, R.B., Heinemeier, J., Bushnell, P.G., Christiansen, J.S., Olsen, J., Ramsey, C.B., et al., 2016. Eye lens radiocarbon reveals centuries of longevity in the Greenland shark (*Somniosus microcephalus*). *Science* 353, 702–704.
- Nielsen, J., 2018. The Greenland shark (*Somniosus microcephalus*). Diet, tracking and radiocarbon age estimates reveal the World's oldest vertebrate. University of Copenhagen. 76, pp.
- Nielsen, J., Christiansen, J.S., Grønkjær, P., Bushnell, P., Steffensen, J.F., Kiilerich, H.O., Præbel, K., et al., 2019. Greenland shark (*Somniosus microcephalus*) stomach contents and stable isotope values reveal an ontogenetic dietary shift. *Front. Mar. Sci.* 6.
- Nosal, A.P., Chao, Y., Farrara, J.D., Chai, F., Hastings, P.A., 2016. Olfaction contributes to pelagic navigation in a coastal shark. *PLoS ONE* 11, 1–17.
- Ona, 1999. Methodology for Target Strength Measurements (With special reference to in situ techniques for fish and mikro-nekton). 65 pp.
- Ona, E., 1990. Physiological factors causing natural variations in acoustic target strength of fish. *J. Marine Biol. Assoc. United Kingdom* 70, 107–127.
- Ona, E., Mitson, R.B., 1996. Acoustic sampling and signal processing near the seabed: The deadzone revisited. *ICES J. Mar. Sci.* 53, 677–690.
- Pedersen, G., Korneliussen, R.J., 2009. The relative frequency response derived from individually separated targets of northeast Arctic cod (*Gadus morhua*), saithe (*Pollachius virens*), and Norway pout (*Trisopterus esmarkii*). *ICES J. Mar. Sci.* 66 (6), 1149–1154.
- Porteiro, F., Sutton, T., Byrkjedal, I., Orlov, A., Heino, M., Menezes, G., Bergstad, O.A., 2017. Fishes of the Northern Mid-Atlantic Ridge Collected During the MAR-ECO Cruise in June-July 2004: An Annotated Checklist. Ponta Delgada. 138pp.
- Simmons, J., MacLennan, D., 2005. Fisheries acoustics: Theory and Practice. Blackwell Science, Oxford, p. 437.
- Simrad, 2012. EK60 reference manual. ISBN: 978-8066-011-4. Issue: 22.03.2012.
- Skomal, G.B., Benz, G.W., 2004. Ultrasonic tracking of Greenland sharks, *Somniosus microcephalus*, under Arctic ice. *Mar. Biol.* 145, 489–498.
- Systat Inc., 1992. Systat for windows: Statistics. SYSTAT, Inc, Evanston.
- Watanabe, Y.Y., Lydersen, C., Fisk, A.T., Kovacs, K.M., 2012. Journal of Experimental Marine Biology and Ecology The slowest fish: Swim speed and tail-beat frequency of Greenland sharks. *Journal of Experimental Marine Biology and Ecology*, 426–427: 5–11. Elsevier B.V. <https://doi.org/10.1016/j.jembe.2012.04.021>.
- Yano, K., Stevens, J.D., Compagno, L.J.V., 2007. Distribution, reproduction and feeding of the Greenland shark *Somniosus (Somniosus) microcephalus*, with notes on two other sleeper sharks, *Somniosus (Somniosus) pacificus* and *Somniosus (Somniosus) antarcticus*. *J. Fish Biol.* 70 (2), 374–390.